A Semi-fluid Multi-functional Binder for High-performance Silicon Anode of Lithium-Ion Batteries

Supporting Information

Hui Xu [a,b,#,*], Xiaoxi Liu [b,c,#], Wenlu Sun [c], Guanghui Xu [b,d], Yihong Tong [b,d], Hongyuan Xu [b,d], Jiawei Li [b,d], Zhao Kong [b,d], Yong Wang [b,e], Zhiyong Lin [c,], Hong Jin [b,d,*], Hongwei Chen [c,*]

a Suzhou Institute of Nano-Tech and Nano-Bionics, Chinese Academic of Sciences, Suzhou, Jiangsu 215123, China
b Xi'an Jiaotong University Suzhou Academy, Suzhou 215123, People's Republic of China
c College of Materials Science and Engineering, Huaqiao University, Xiamen 361021, People's Republic of China
d Nano Science and Technology Institute, University of Science and Technology of China, Suzhou, Jiangsu 215123, China
e State Key Laboratory for Mechanical Behaviour of Materials, Xi'an Jiaotong University, Xi'an, Shaanxi 710049, People's Republic of China
# These authors contributed equally to this work and should be considered co-first authors.
*E-mail: xhxuhui@xjtu.edu.cn; jhjinhong@mail.xjtu.edu.cn; hwchen@hqu.edu.cn

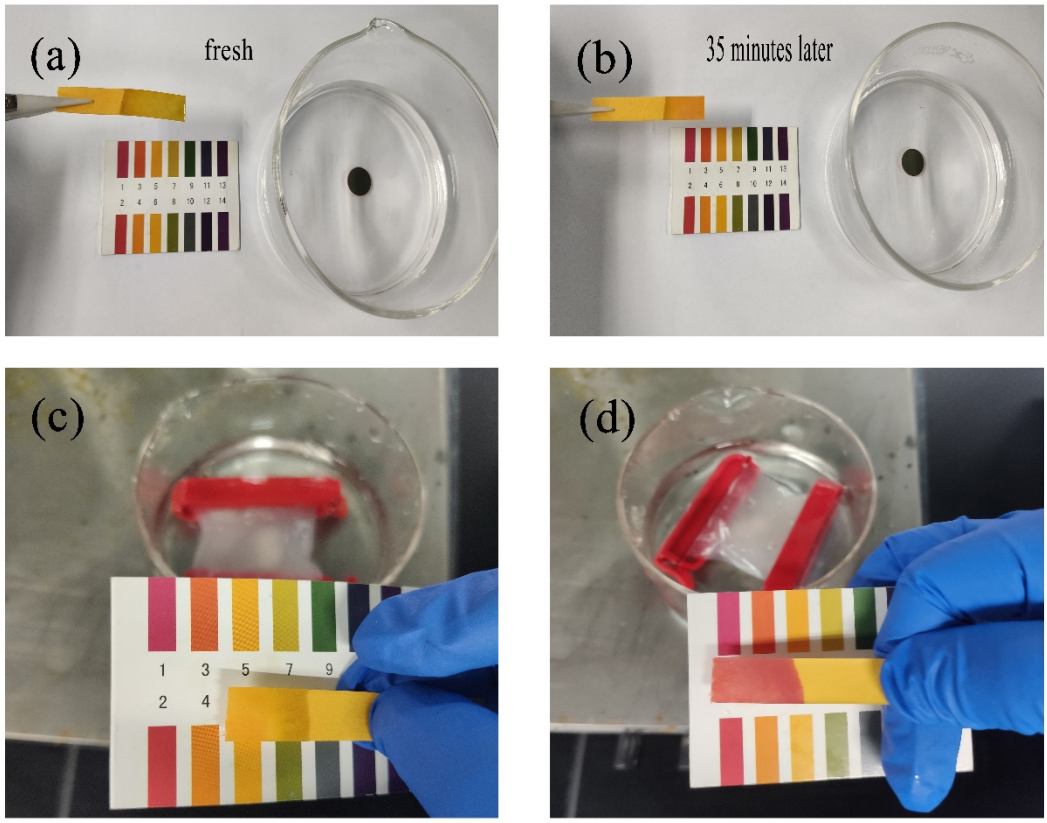

Figure S1. The PH for the verification of dissociative CA. (a) the fresh Si@GPC electrode, (b) Letting the electrode stand for 35 minutes, (c) the GPC binder on the dialysis bag, (d) Letting the GPC binder stand for 35 minutes.

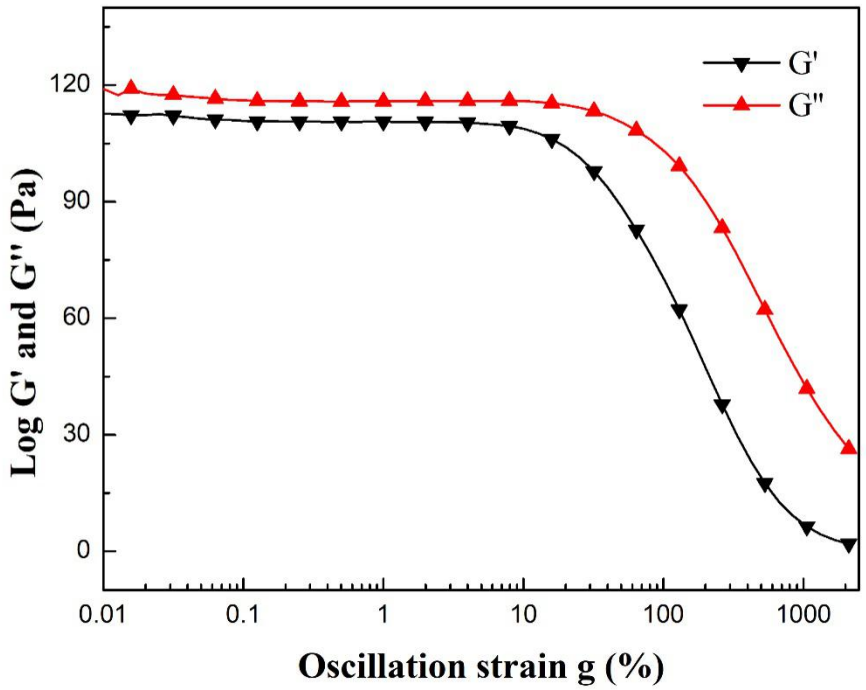

Figure S2. The rheological response of GPC binder.

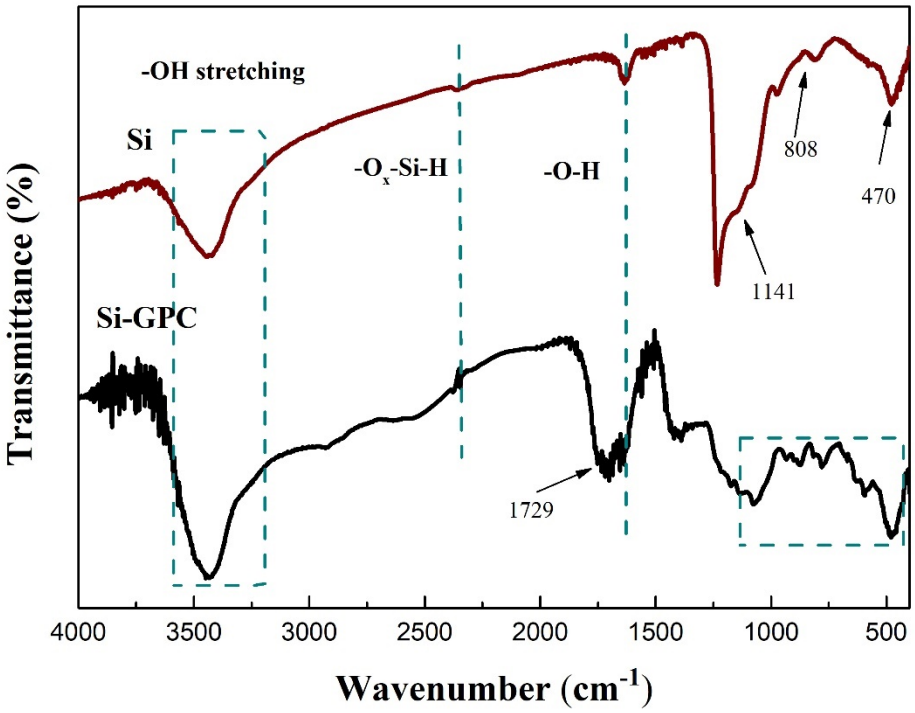

Figure S3. FTIR spectra of Si particles and Si-GPC binder.

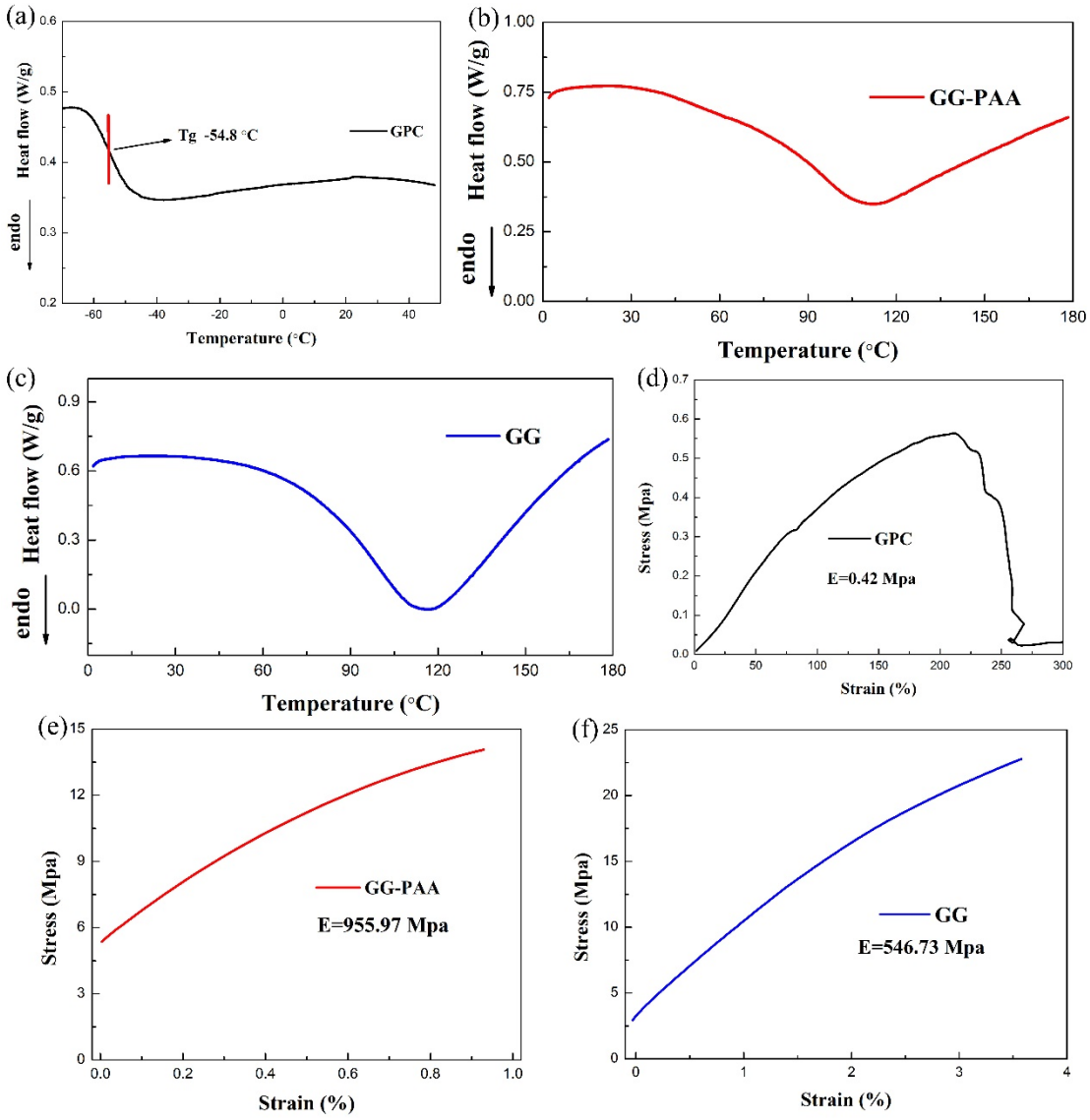

Figure S4. The thermal property and mechanical performance of the GPC, GG-PAA, GG binder. DSC curves of (a) GPC, (b) GG-PAA and (c) GG binder; Stress-strain curves of (d)GPC, (e) GG-PAA and (f) GG by DMA.

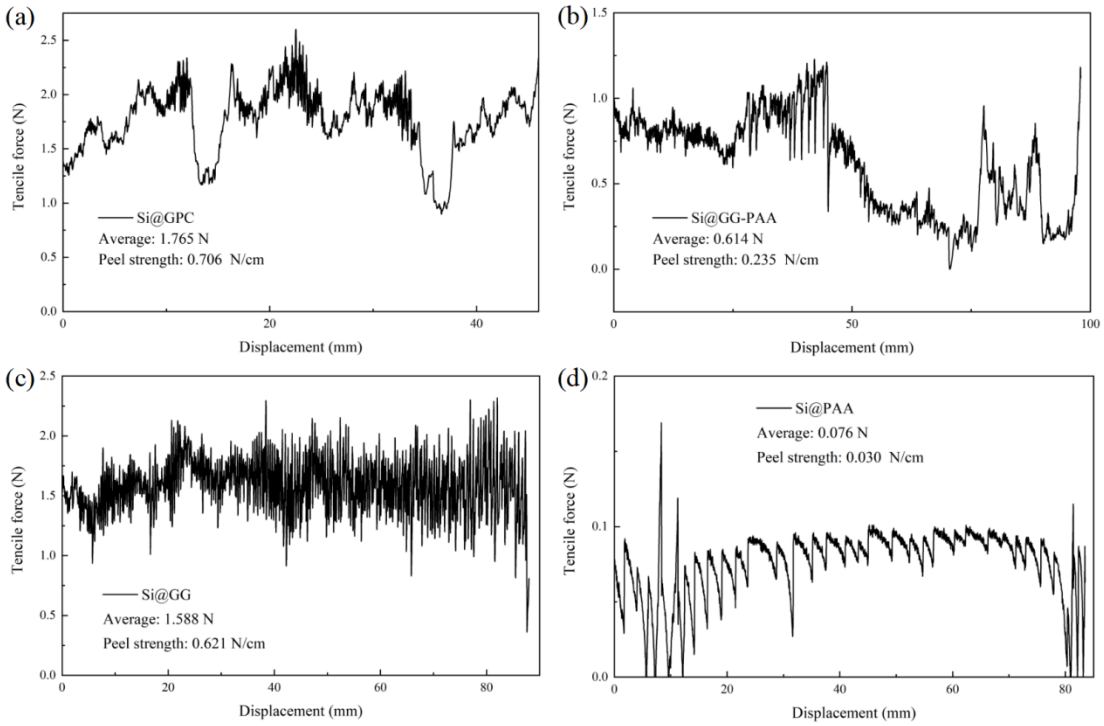

Figure S5. Peel curves of (a) Si@GPC, (b) Si@GG-PAA, (c) Si@GG and (d) Si@PAA anode.

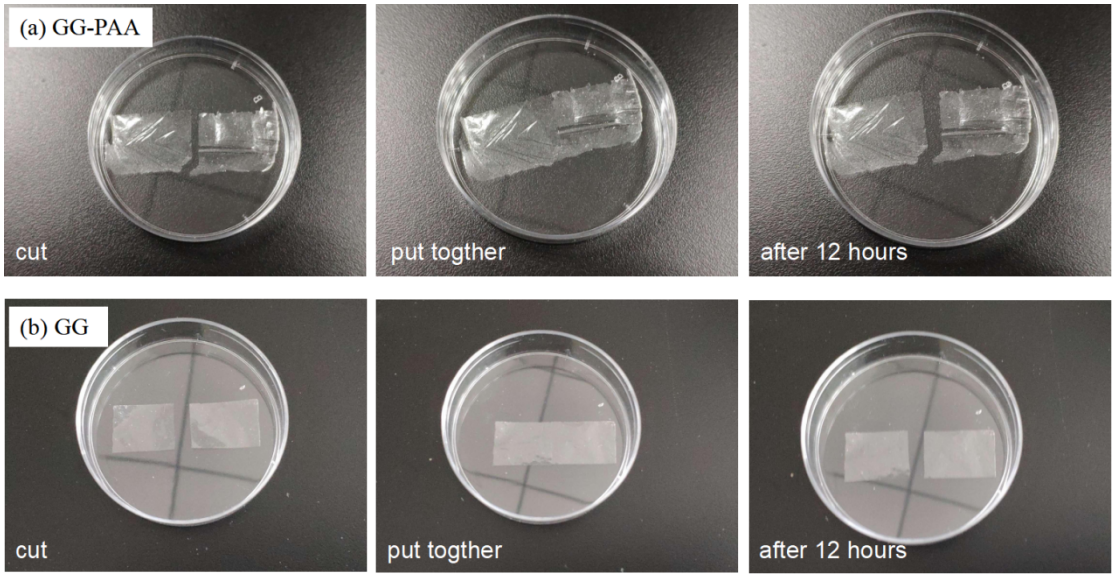

Figure S6. Self-healing test of the (a) GG-PAA and (b) GG binder.

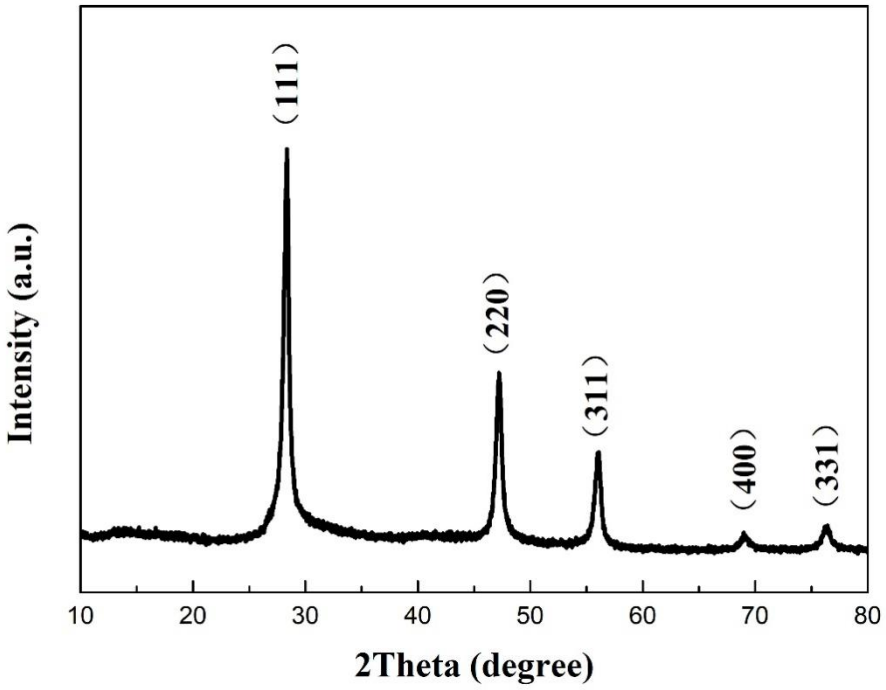

Figure S7. XRD patterns of the Si nanoparticles.

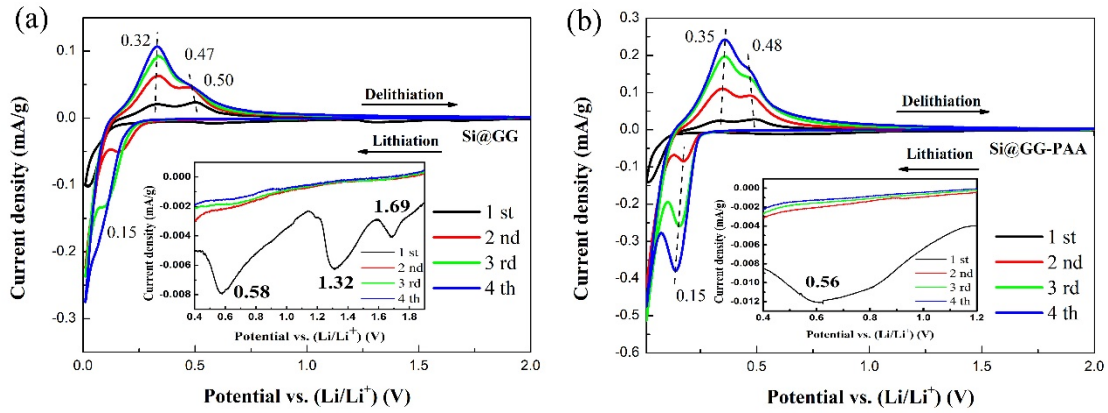

Figure S8. CV curves of (a) Si@GG electrode and (b) Si@GG-PAA electrode at the scan rate of 0.02 mV s^{-1}.

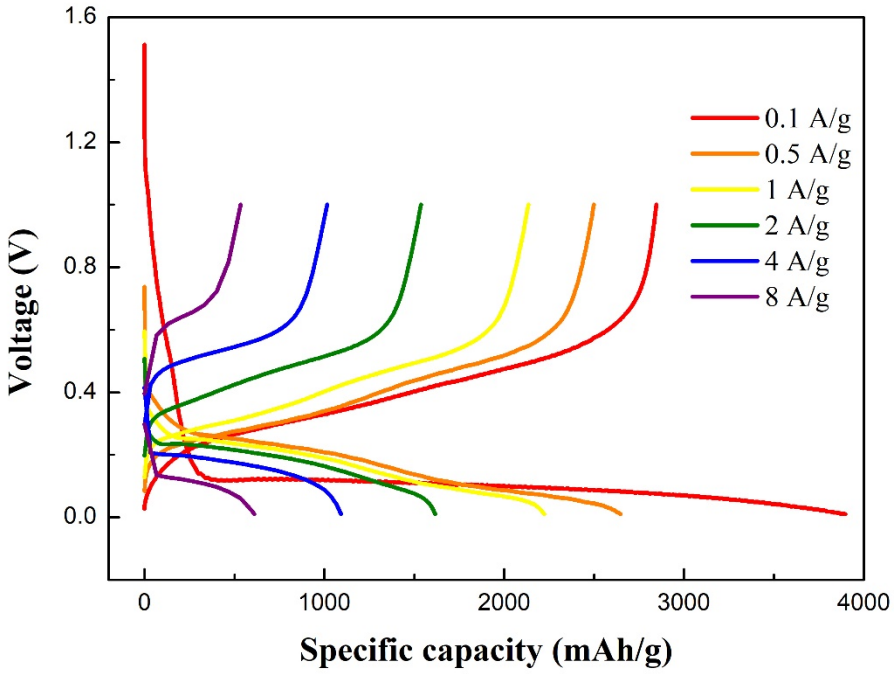

Figure S9. The discharge/charge profiles of the Si@GPC electrode.

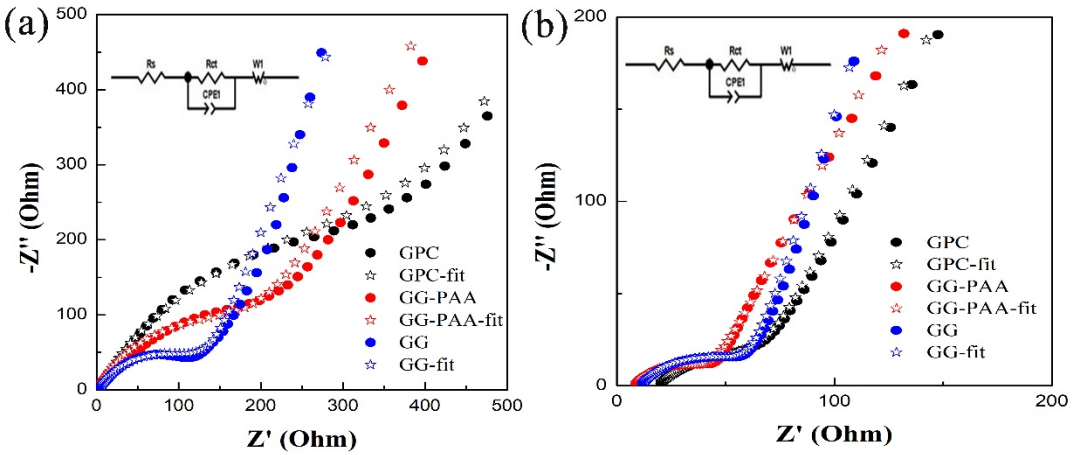

Figure S10. (a) EIS plots of Si electrodes with different binders of fresh cycle. (b) EIS plots of Si electrodes with different binders after 100 cycles.

Table S1 The D_{Li}^{+} of Si@GPC during the lithiation/delithiation processes.

Lithiation	τ/s	ΔEs/V	ΔEt/ V	D/ cm^2 s^{-1}
10	1800	0.018	0.0853	3.75×10^{-10}
20	1800	0.0074	0.0645	1.11×10^{-10}
30	1800	0.0071	0.0607	1.15×10^{-10}
40	1800	0.0099	0.062	2.15×10^{-10}
50	1800	0.0158	0.062	5.47×10^{-10}
60	1800	0.0078	0.0517	1.92×10^{-10}
70	1800	0.0047	0.0471	0.84×10^{-10}
80	1800	0.0035	0.0453	0.50×10^{-10}
90	1800	0.004	0.0483	0.58×10^{-10}
Delithiation	τ/s	ΔEs/V	ΔEt/ V	D/ cm^2 s^{-1}
10	1800	0.0152	0.045	9.61×10^{-10}
20	1800	0.0084	0.0413	3.48×10^{-10}
30	1800	0.0077	0.0421	2.82×10^{-10}
40	1800	0.0087	0.0456	3.07×10^{-10}
50	1800	0.0114	0.0512	4.18×10^{-10}
60	1800	0.0115	0.0527	4.01×10^{-10}
70	1800	0.0077	0.0524	1.82×10^{-10}
80	1800	0.0087	0.0598	1.78×10^{-10}
90	1800	0.0139	0.0865	2.18×10^{-10}

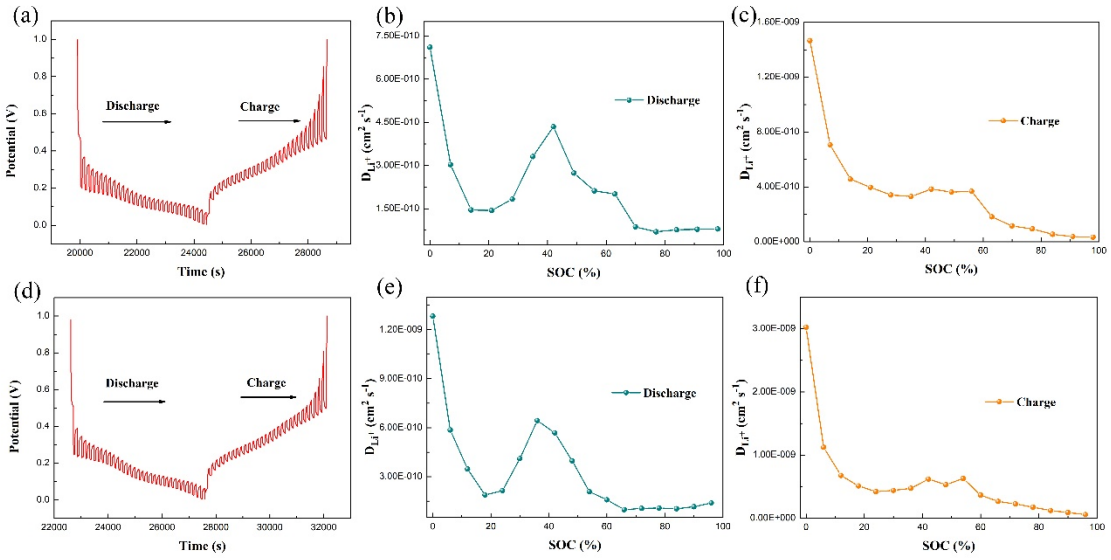

Figure S11. (a) and (d) the GITT curves (voltage vs. time) for the Si@GG and Si@GG-PAA electrode at room temperature. (b-c) during the lithiation processes for the Si@GG

and Si@GG-PAA electrode. (e-f) D_{Li^+} during the delithiation processes for the Si@GG and Si@GG-PAA electrode.